PROCEEDINGS OF SCIENCE

SK-Gd as an Observatory of Stars (Sun & Supernovæ)

Antoine Beauchêne[a,†,*] **on behalf of the Super-Kamiokande Collaboration**

[a] *École polytechnique, Laboratoire Leprince-Ringuet, CNRS, F-91120, Palaiseau, France*

E-mail: antoine.beauchene@llr.in2p3.fr

Super-Kamiokande is a 50 kton water Cherenkov detector located in Japan, currently the largest in the world. This makes it an ideal observatory for studying neutrinos originating from stars. Among other capabilities, it enables the observation of ^{8}B solar neutrinos by analysing the effects of MSW resonances in the Sun and the Earth on their spectrum and flux, respectively. It also allows for the study of neutrinos produced during core-collapse supernovæ as well as the diffuse supernova neutrino background. The recent addition of gadolinium into the tank has enhanced these studies by improving the identification of neutron captures. The results of these analyses are summarised here.

12th Neutrino Oscillation Workshop (NOW2024)
2-8, September 2024
Otranto, Lecce, Italy

*Speaker

†Has now moved to University of Oxford, Department of Physics, Oxford, United Kingdom.

https://pos.sissa.it/

PoS(NOW2024)067

1. Introduction

The **S**uper-**K**amiokande (SK) detector is a 50 ktons water Cherenkov detector that started taking data in April 1996. It is located 1 000 m (equivalent to 2.7 km of water) underground in the Kamioka mine in Japan, to shield it from cosmic muons. With a fiducial volume of 22.5 ktons of ultrapure water, SK is equipped with 11 129 **P**hoto**M**ultiplier **T**ubes (PMTs) of 50 cm in diameter in its inner part that allow it to detect the faint flashes of Cherenkov light produced by charged particles in water travelling at a speed greater than the speed of light in this medium. These particles are typically generated as a result of interactions between neutrinos and the water molecules, enabling the detector to probe fundamental questions in particle physics and astrophysics.

Neutrinos, being nearly massless and electrically neutral, interact only weakly with matter, making their detection extraordinarily challenging but rewarding. Among the various existing sources of neutrinos, stars are a significant one. They generate an enormous number of neutrinos throughout their lifetime, primarily produced through two sets of nuclear reactions: the *pp* chain and the CNO cycle. Their relative proportions vary depending on the star's mass; in the case of the Sun, the CNO cycle accounts for less than 1% of the total energy and the production of electron neutrinos.

Measurements of the flux of these neutrinos by the SK [1] and the **S**udbury **N**eutrino **O**bservatory (SNO) [2] experiments have confirmed the deficit observed by Homestake [3] while also verifying the predictions of the **S**tandard **S**olar **M**odel (SSM) [4]. This deficit cannot be explained solely by vacuum oscillations, it is necessary to consider the propagation of neutrinos in the Sun's dense matter, which enhances oscillations through the **M**ikheyev-**S**mirnov-**W**olfenstein (MSW) resonance [5–7] for neutrinos with energies above $\mathcal{O}(1)$ MeV. Due to its energy detection threshold of around 3 MeV, SK is primarily sensitive to neutrinos generated by the decay of ^{8}B, while others are produced in the *pp*, *pep*, ^{7}Be, *hep* processes, and the CNO cycle.

When a star reaches the end of its life, if its mass is at least eight times that of the Sun, it will undergo a **C**ore-**C**ollapse **S**uper**N**ova (CCSN), leaving behind a neutron star or a black hole. During this process, 10^{58} neutrinos of approximately 10 MeV across all flavours are released, corresponding to 99% of the total emitted energy. Detecting these neutrinos would allow us to better understand the processes at work in the CCSN mechanism. However, the event must be sufficiently close to detect a significant number in SK. Typically, in the Milky Way, the predicted rate is 1 to 2 per century [8].

Since neutrinos can escape from the stellar core faster than photons, we could detect some of these pre-CCSN neutrinos before the photons. Thus, in addition to providing insights into neutrinos and the CCSN mechanism, they could serve as early alerts for a nearby CCSN [9, 10].

As we anticipate the next transient event, SK is uniquely positioned to explore the **D**iffuse **S**upernova **N**eutrino **B**ackground (DSNB) [11], a faint flux of neutrinos originating from all past CCSNe in the universe. The DSNB provides a window into the history of stellar evolution and CCSN rate, as well as an opportunity to test cosmological models and exotic neutrino properties.

In 2020 and 2022, **Gad**olinium (Gd) in the form of gadolinium sulphate octahydrate has been introduced into the water at a Gd concentration of 0.01% and 0.03% by mass respectively [12, 13], allowing the enhancement of the neutron tagging efficiency for **I**nverse **B**eta **D**ecay (IBD) events. The main interaction channel for the detection of DSNB in SK is IBD, for which SK has published the most stringent upper limits using data up to SK-IV [14], as well as more recently for the first Gd-loaded phase [15].

Here, we review the capabilities of SK as a multi-purpose observatory of neutrinos from both the Sun and the DSNB. Particular attention is given to the role of the SK-Gd upgrade in advancing the detection prospects for the DSNB, marking a new era in neutrino astrophysics.

2. Solar Neutrinos

In SK, solar neutrinos are studied using electron elastic scattering, enabling us to reconstruct their direction precisely and pinpoint their source:

$$\nu_\alpha + e^- \to \nu_\alpha + e^- \tag{1}$$

where $\alpha \in \{e, \mu, \tau\}$. Although all three flavours are involved in this process, it is around 6 times more sensitive to the electronic flavour because it can interact via CC and NC.

Depending on the time of day, these neutrinos may also travel through the Earth, leading to a second MSW resonance and the regeneration of the electron flavour. This effect is studied by comparing the flux of solar neutrinos observed during the day to that measured at night, as illustrated in Figure 1a, thereby defining a day/night asymmetry factor:

$$A_{\mathrm{D/N}} = \frac{\Phi^{\mathrm{day}}_{^8\mathrm{B}} - \Phi^{\mathrm{night}}_{^8\mathrm{B}}}{\frac{1}{2}(\Phi^{\mathrm{day}}_{^8\mathrm{B}} + \Phi^{\mathrm{night}}_{^8\mathrm{B}})} \tag{2}$$

The SK-IV phase thus highlights an asymmetry of:

$$A^{\mathrm{SK-IV,\,fit}}_{\mathrm{D/N}} = -0.0262 \pm 0.0107\,(\mathrm{stat.}) \pm 0.0030\,(\mathrm{sys.}) \tag{3}$$

By extending this analysis to previous phases, this asymmetry is measured for each of them, with the results presented in Figure 1b. Then, combining the data from phases I to IV yields the following result:

$$A^{\mathrm{SK,\,fit}}_{\mathrm{D/N}} = -0.0286 \pm 0.0085\,(\mathrm{stat.}) \pm 0.0032\,(\mathrm{sys.}) \tag{4}$$

This result allows us to reject, for the first time, the case of no asymmetry at the $3.2\,\sigma$ level, thus providing evidence in favour of a matter effect during the propagation of solar neutrinos through the Earth.

Moreover, one can probe the so-called *upturn* region, where the survival probability of electron neutrinos increases with energy due to matter effects in the Sun. To analyse the shape of the energy spectrum (Figure 2), a fit to quadratic, cubic, and exponential functions is performed, taking into account correlations between SK phases and energy bins. The SK data allow us to reject the hypothesis of no upturn at the $1.2\,\sigma$ level. By combining these data with those from SNO, a distorted spectrum is favoured at the $2.1\,\sigma$ level.

Finally, a global oscillation analysis was performed, combining the results from SK-I, II, III, and IV phases with those from the SNO, Borexino, and radiochemical experiments (Homestake,

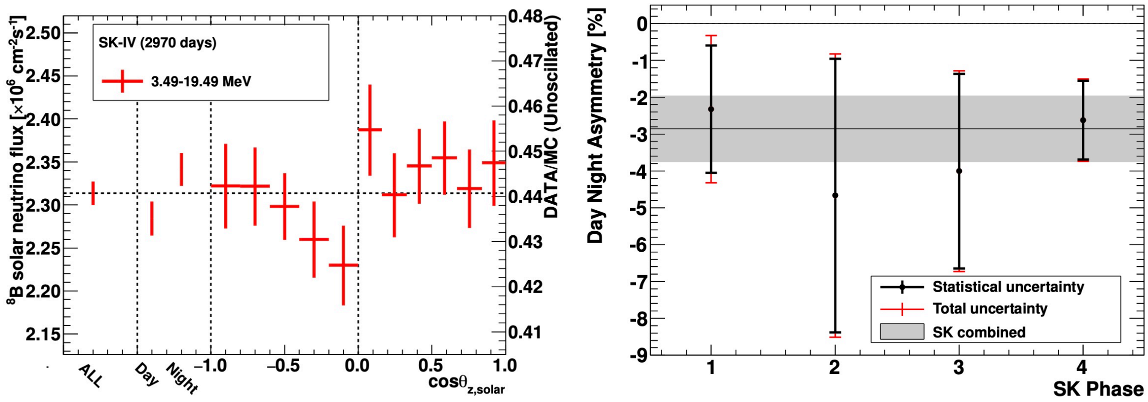

(a) Measurements of the solar neutrino flux of ^{8}B in SK-IV as a function of the solar zenith angle

(b) Values for the different SK phases as well as the combined value

Figure 1: Results of the day/night asymmetry analysis

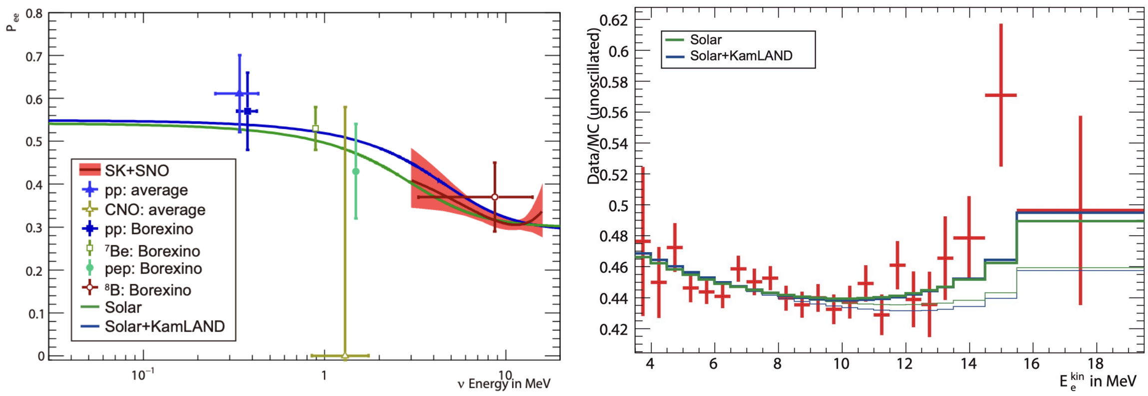

(a) Quadratic fit result of SK+SNO to the electron neutrino survival probability as a function of neutrino energy

(b) Binned data from the combination of SK-I to IV phases

Figure 2: Results of the energy spectrum analysis (upturn)

Gallex/GNO, and SAGE). These results are compared and combined with those obtained by the reactor electron antineutrino experiment KamLAND, which, unlike the former experiments that are primarily sensitive to $\sin^2(\theta_{12})$, is more sensitive to Δm^2_{21}.

The best-fit contours for the different configurations are shown in Figure 3, highlighting a 1.5 σ tension in the best-fit values of Δm^2_{21} obtained from the global solar analysis and KamLAND. This tension could be explained, for instance, by CPT symmetry violation if it is confirmed.

The preliminary analysis of solar neutrinos in the phases following SK-IV has allowed for an estimation of the ^{8}B solar neutrino flux observed in the latest SK phases, including the Gd-doped SK-VI and VII phases. The results, presented in Table 1, are comparable to those previously published from the combination of SK-I to IV phases.

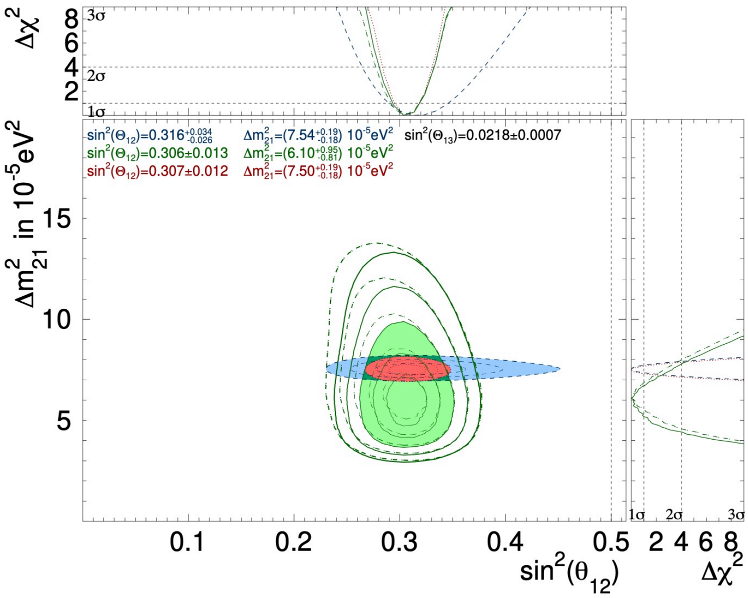

Figure 3: Best-fit contours for $\sin^2(\theta_{12})$ and Δm^2_{21} from the global solar analysis (green) at $1-5\,\sigma$, KamLAND (blue) at $1-3\,\sigma$, as well as the combined global solar + KamLAND result (red). The results from the SK + SNO combination are also shown with dashed-dotted contours.

Phase	Data/MC	Flux $[10^6\,\mathrm{cm^{-2}\cdot s^{-1}}]$
SK-I→IV	0.445 ± 0.002 ± 0.008	2.336 ± 0.011 ± 0.043
SK-V	0.445 ± 0.010	2.34 ± 0.04
SK-VI	0.436 ± 0.009	2.29 ± 0.05
SK-VII	0.446 ± 0.010	2.34 ± 0.05

Table 1: Summary of the measured ^{8}B solar neutrino fluxes. For SK-I→IV, the first uncertainty is statistical and the second is systematic, whereas for the other phases, only statistical uncertainties are given

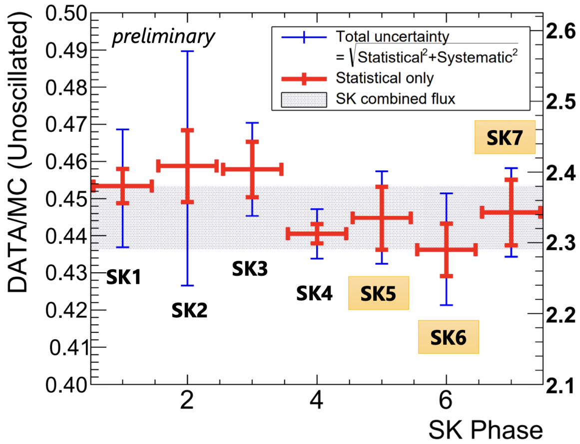

Figure 4: Comparison of the ^{8}B solar neutrino fluxes across different SK phases, with the combined SK-I to IV result shown as a grey band

3. Diffuse Supernova Neutrino Background

Regarding the DSNB, a revisited version of previous analyses [14] has been developed, aiming to highlight a potential DSNB excess using an unbinned fitting approach that adjusts the predictions of the background sources and the DSNB signal ($\boldsymbol{N}_b,\ N_s$) to the data from various SK phases. This analysis includes, for the first time, the SK-Gd phases (552.2 and 404.0 livedays for SK-VI and VII, respectively). To achieve this, the following extended likelihood function is maximised:

$$\mathcal{L}(\boldsymbol{E}|N_s,\ \boldsymbol{N}_b, \boldsymbol{\varepsilon}) = \mathcal{L}(\boldsymbol{\varepsilon}_0|\boldsymbol{\varepsilon}) \cdot e^{-\sum_{j\in s+b} N_j} \prod_{i=1}^{N_{\text{data}}} \sum_{j\in s+b} N_j \cdot \text{PDF}_j\,(E^i,\ \theta_C^i,\ N^i_{\text{tagged }n}|\boldsymbol{\varepsilon}) \qquad (5)$$

where $\boldsymbol{\varepsilon}$ is the vector of nuisance parameters accounting for systematic uncertainties (of both signal and backgrounds), $\mathcal{L}(\boldsymbol{\varepsilon}_0|\boldsymbol{\varepsilon})$ is their **P**robability **D**ensity **F**unction (PDF), and PDF_j corresponds to the PDF of a given category j (signal or background) in the space of the relevant parameters.

To fully exploit the two daughter particles from IBD ($\bar{\nu}_e + p \to e^+ + n$), the parameter space has been divided into six regions:

- Three angular regions based on the reconstructed Cherenkov angle θ_C associated with the positron, e.g. $\theta_C \in [38°,\ 53°[$, along with two sidebands;
- These regions are further subdivided into two categories based on the number of neutrons tagged by our machine learning algorithms: $N_{\text{tagged }n} = 1$ or $\neq 1$.

Being dominated at low energies by spallation (as well as reactor neutrinos), the fit is performed for each SK phase considered in the analysis between 16 and 80 MeV in reconstructed positron energy. Assuming the DSNB model from [11] for the construction of the signal PDF, Figure 5 shows the profiled likelihood ratio functions for the different SK phases as well as their combination. The best combined fit associated with the annual DSNB event rate in the fiducial volume of SK is $2.86^{+1.62}_{-1.27}$ events $\cdot$ (22.5 ktons)$^{-1}$ $\cdot$ year^{-1}, corresponding to an electron antineutrino flux of $1.44^{+0.82}_{-0.64}\ \text{cm}^{-2} \cdot \text{s}^{-1}$ (for $E_e > 16\,\text{MeV} \Leftrightarrow E_\nu > 17.3\,\text{MeV}$). This value represents an excess of $2.27\,\sigma$ over the background-only hypothesis. A 90% confidence level upper limit on the DSNB flux is also inferred which results in a value of $2.55\,\text{cm}^{-2} \cdot \text{s}^{-1}$ (for $E_\nu > 17.3\,\text{MeV}$).

This procedure is then repeated for various DSNB models, but being currently limited by statistics, this model-dependent analysis yields results that remain relatively independent of the assumed model.

A second DSNB analysis is conducted, this time binned and model-dependent. It focuses on the region of the signal parameter space, i.e. central θ_C and $N_{\text{tagged }n} = 1$, and derives upper limits in each bin. As shown in Figure 6, the combination of SK-VI and VII phases, despite being approximately three times shorter than SK-IV, allows for upper limits comparable to the latter, illustrating how Gd enhances our sensitivity.

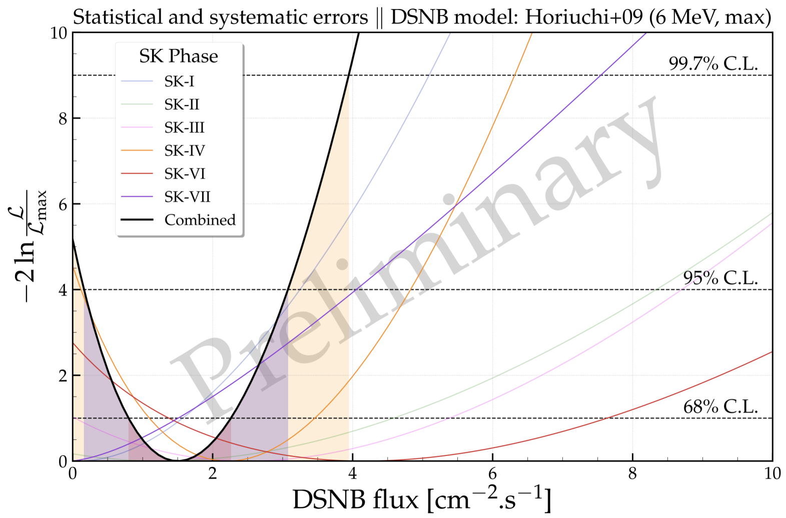

Figure 5: Profiled likelihood ratio as a function of the DSNB flux for the different SK phases and their combination, assuming the DSNB model from [11]. The red, purple, and yellow bands correspond to the 68%, 95%, and 99.7% confidence levels, respectively.

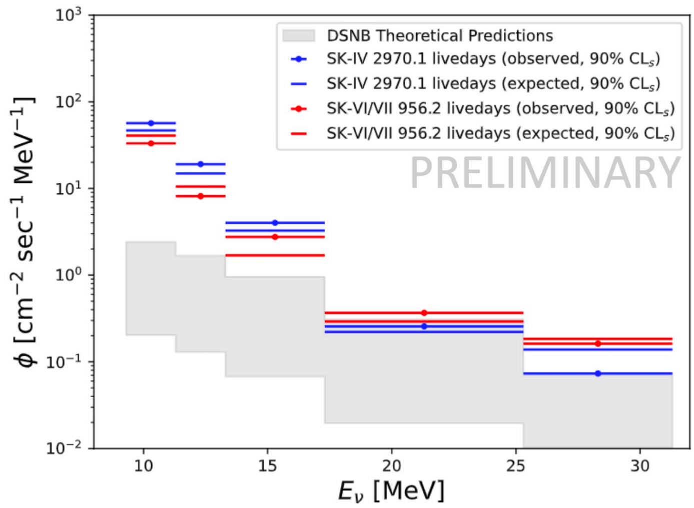

Figure 6: Upper limits with expected sensitivities for SK-IV as well as for the combination of phases SK-VI and VII

4. Conclusion

SK is therefore a leading observatory for probing both solar and CCSNe physics. The results of the solar neutrino analysis allow, for the first time, the rejection of the hypothesis of no day/night asymmetry in the ^{8}B solar neutrino flux due to matter effects in the Earth at 3.2 σ. Furthermore, the results of the *upturn* region analysis, combining SK and SNO data, enable the rejection of the no-upturn hypothesis at 2.1 σ.

Finally, the model-dependent unbinned DSNB analysis of SK data, incorporating for the first time the Gd-doped phases, allows the rejection of the background-only hypothesis at 2.3 σ while continuing to set the world's most stringent upper limits.

References

[1] J. Hosaka *et al.* (Super-Kamiokande Collaboration), *Solar neutrino measurements in Super-Kamiokande-I*, *Phys. Rev. D* **73**, 112001 (2006).

[2] Q. R. Ahmad *et al.* (SNO Collaboration), *Measurement of the Rate of* $\nu_e + d \to p + p + e^-$ *Interactions Produced by* ^{8}B *Solar Neutrinos at the Sudbury Neutrino Observatory*, *Phys. Rev. Lett.* **87**, 071301 (2001).

[3] R. Davis, D. S. Harmer and K. C. Hoffman, *Search for Neutrinos from the Sun*, *Phys. Rev. Lett.* **20**, 1205 (1968).

[4] J. N. Bahcall, N. A. Bahcall and G. Shaviv, *Present Status of the Theoretical Predictions for the* ^{37}Cl *Solar-Neutrino Experiment*, *Phys. Rev. Lett.* **20**, 1209 (1968).

[5] L. Wolfenstein, *Neutrino oscillations in matter*, *Phys. Rev. D* **17**, 2369 (1978).

[6] S. P. Mikheyev and A. Y. Smirnov, *Resonance enhancement of oscillations in matter and solar neutrino spectroscopy*, *Sov. J. Nucl. Phys.* **42**, 913 (1985).

[7] S. P. Mikheyev and A. Y. Smirnov, *Resonant amplification of neutrino oscillations in matter and solar neutrino spectroscopy*, *Nuovo Cim. C* **9**, 17 (1986).

[8] K. Rozwadowska, F. Vissani and E. Cappellaro, *On the rate of core collapse supernovae in the milky way*, *New Astron.* **83**, 101498 (2021).

[9] L. N. Machado *et al.* (Super-Kamiokande Collaboration), *Pre-supernova Alert System for Super-Kamiokande*, *ApJ* **935**, 40 (2022).

[10] Y. Kashiwagi *et al.* (Super-Kamiokande Collaboration), *Performance of SK-Gd's Upgraded Real-time Supernova Monitoring System*, *ApJ* **970**, 93 (2024).

[11] S. Horiuchi, J. F. Beacom and E. Dwek, *Diffuse supernova neutrino background is detectable in Super-Kamiokande*, *Phys. Rev. D* **79**, 083013 (2009).

[12] K. Abe *et al.* (Super-Kamiokande Collaboration), *First gadolinium loading to Super-Kamiokande*, *Nucl. Instrum. Meth. A* **1027**, 166248 (2022).

[13] K. Abe *et al.* (Super-Kamiokande Collaboration), *Second gadolinium loading to Super-Kamiokande*, *Nucl. Instrum. Meth. A* **1065**, 169480 (2024).

[14] K. Abe *et al.* (Super-Kamiokande Collaboration), *Diffuse supernova neutrino background search at Super-Kamiokande*, *Phys. Rev. D* **104**, 122002 (2021).

[15] M. Harada *et al.* (Super-Kamiokande Collaboration), *Search for Astrophysical Electron Antineutrinos in Super-Kamiokande with 0.01% Gadolinium-loaded Water*, *ApJL* **951**, L27 (2023).

[16] K. Abe *et al.* (Super-Kamiokande Collaboration), *Solar neutrino measurements using the full data period of Super-Kamiokande-IV*, *Phys. Rev. D* **109**, 092001 (2024).